

Testing and stability analysis of modified gravity theories

László Árpád Gergely

University of Szeged



based on:

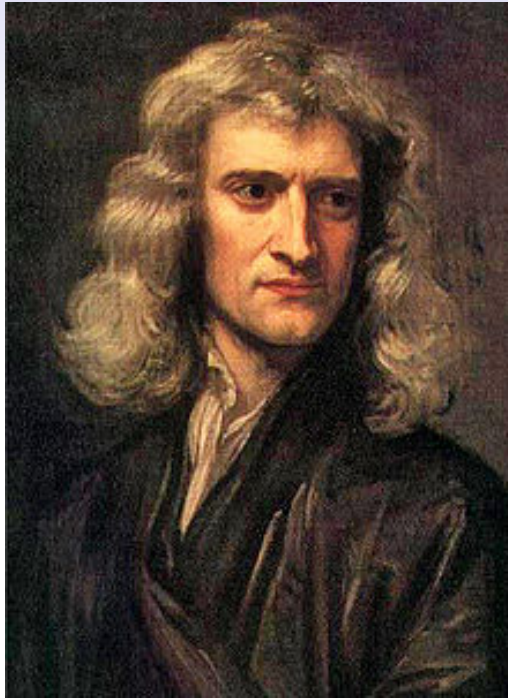
R. Kase, L. Á. Gergely, S. Tsujikawa, Phys. Rev. D 90, 124019 (2014)

C. Gergely, Z. Keresztes, L. Á. Gergely, Phys. Rev. D, in press (2019)

Modern Theories of Gravitation

Hungarian Academy of Sciences

Isaac Newton: the first successful gravity theory



1642 - 1726/7

Philosophiæ Naturalis Principia Mathematica (1687)

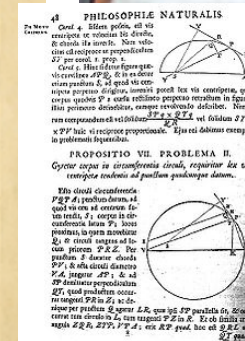
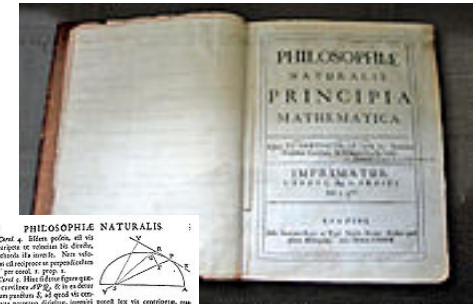
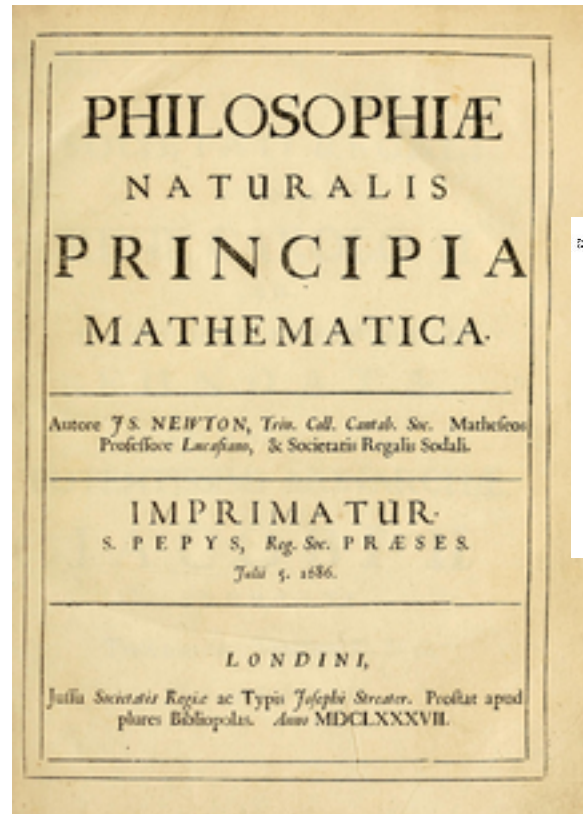
Establishes classical mechanics

Three laws of motion

Universal gravity theory

Derives Kepler's laws

Develops Calculus



Newton's gravity theory: strengths and limitations

Strengths:

Unique logical framework for both the celestial and everyday life motions

Powerful tool, allowing Le Verrier to predict the planet Neptune from the motion of the planet Uranus

Remarkably precise on the Earth (for weak gravity and slow motions)

$$\varepsilon = \frac{Gm}{c^2 r} \approx \frac{v^2}{c^2} \ll 1$$

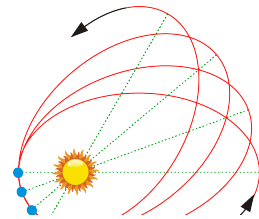
Simple: one single scalar field

Limitations:

Assumes aether



The motion of the planets deviates from the Newtonian prediction (excess in the perihelion shift)



Not precise enough even on the Earth if one desires to use GPS

its accuracy of 15 m requires 50 ns temporal precision

SR: time dilation

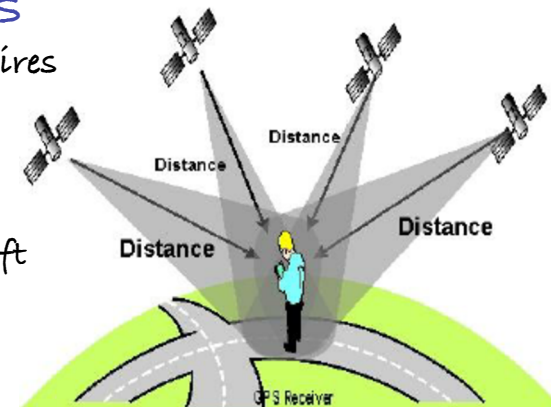
-7 μs / day

GR: gravitational blueshift

45 μs / day

Combined inaccuracy of

11.4 km / day

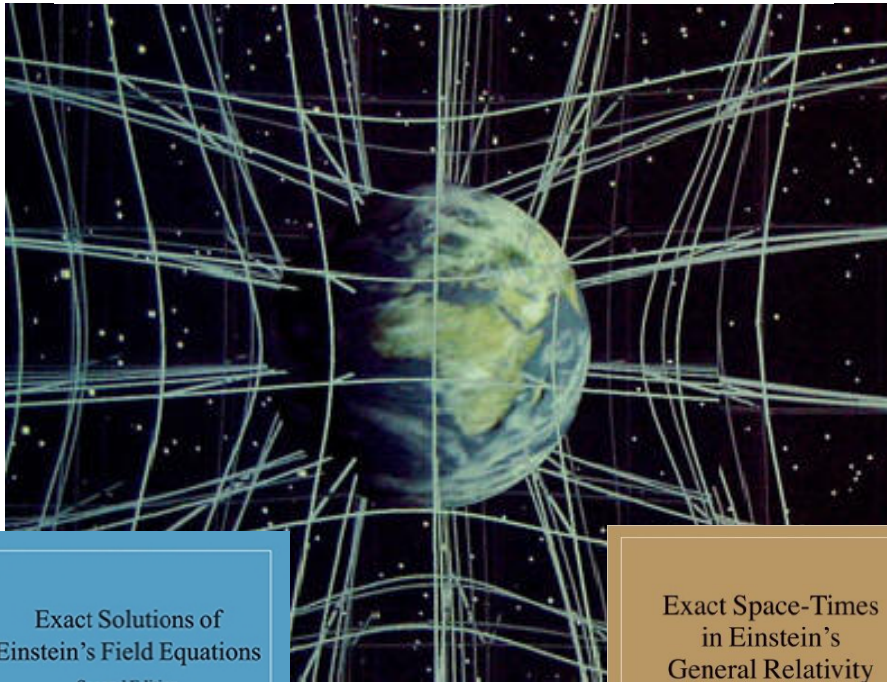


Infinite propagation speed

General relativity, Einstein's gravity theory

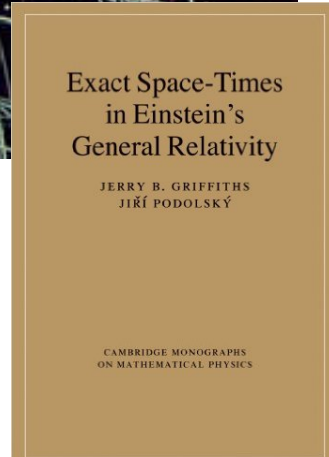
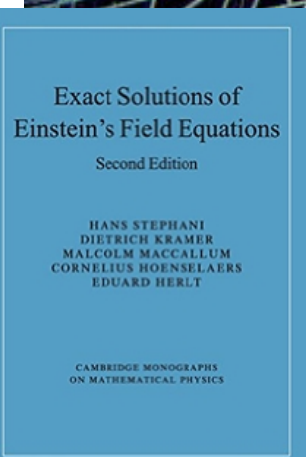
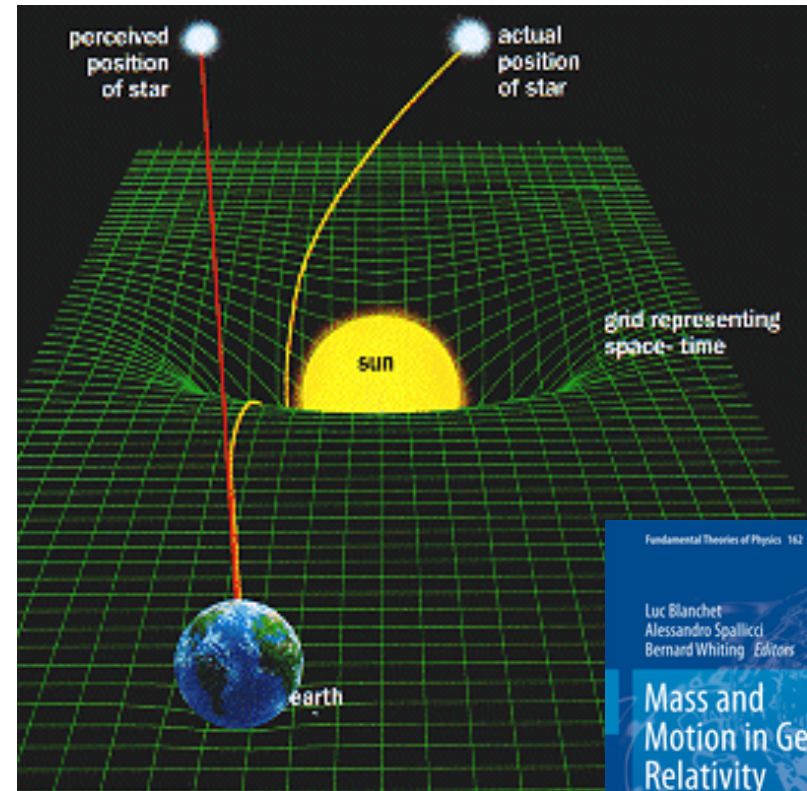
1. Matter tells space-time how to curve
(Einstein equation)

$$R_{\mu\nu} - \frac{1}{2}R g_{\mu\nu} + \Lambda g_{\mu\nu} = \frac{8\pi G}{c^4} T_{\mu\nu}$$



2. Space-time tells matter, how to move
(geodesic equation)

$$\frac{d^2 x^\mu}{ds^2} = -\Gamma^\mu_{\alpha\beta} \frac{dx^\alpha}{ds} \frac{dx^\beta}{ds}$$



The success of General Relativity

Solar System & other tests

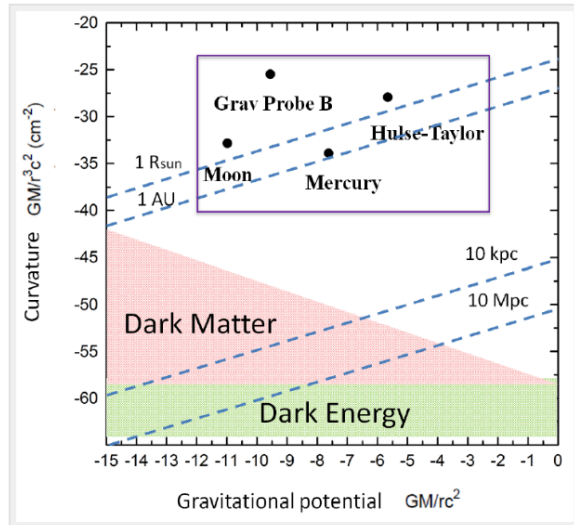
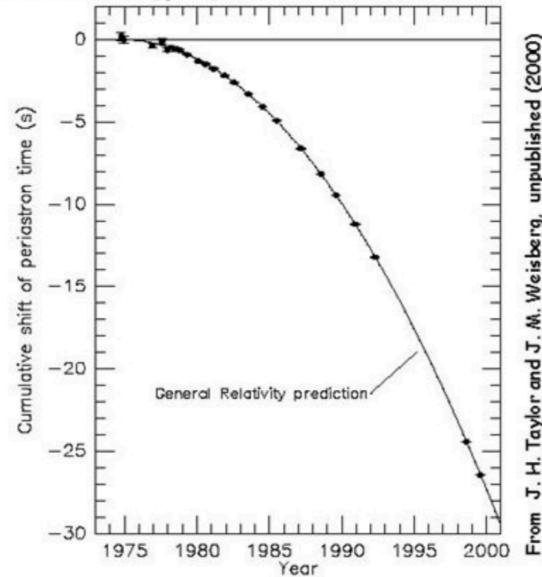


Fig 1: Tests of General Relativity on various scales. The vertical axis is the spacetime curvature and the horizontal axis is the gravitational potential. The blue dotted lines indicate typical length scales. Modified from Psaltis arXiv:0806.1531. GR is well tested at solar system scales and also by binary pulsars (within the purple box). However, outside this region, gravity is not tested by conventional methods.

www.icg.port.ac.uk/cosmological-tests-of-gravity/

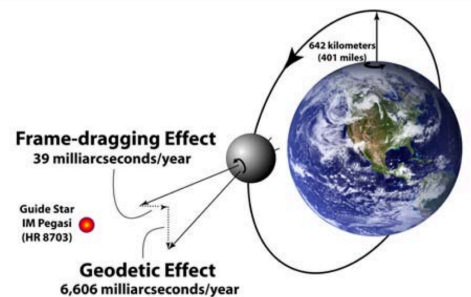
Hulse-Taylor pulsar

Comparison between observations of the binary pulsar PSR1913+16, and the prediction of general relativity based on loss of orbital energy via gravitational waves



40s change in 30 years!! (4×10^{-8})

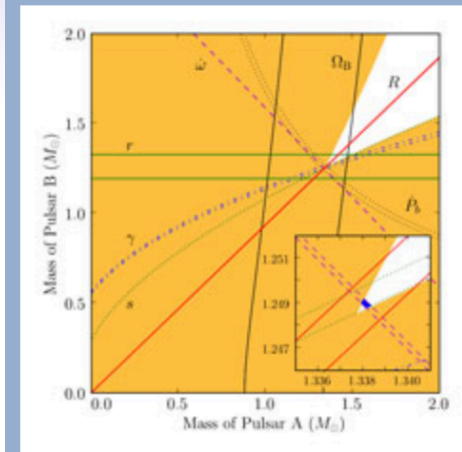
Gravity Probe B



Everitt, C.W.F.; Parkinson, B.W. (2009).

"Gravity Probe B Science Results—NASA Final Report"

Double pulsar



Mass-mass diagram illustrating the present tests constraining general relativity in the double pulsar PSR J0737-3039A/B. Because observations are consistent with general relativity, all lines intersect at common values of masses. Shaded orange regions are unphysical solutions because $\sin i \leq 1$, where i is the orbital inclination. The mass ratio, R , and five post-Keplerian parameters (s and r , Shapiro delay shape and range; ω , periastron advance; P_b , orbital period decay due to the emission of gravitational waves; and γ , gravitational redshift and time dilation) were reported by Kramer et al. (2006). The spin precession rate of pulsar B, Ω_B , yields a new constraint on the mass-mass diagram.

The success of General Relativity: Gravitational waves

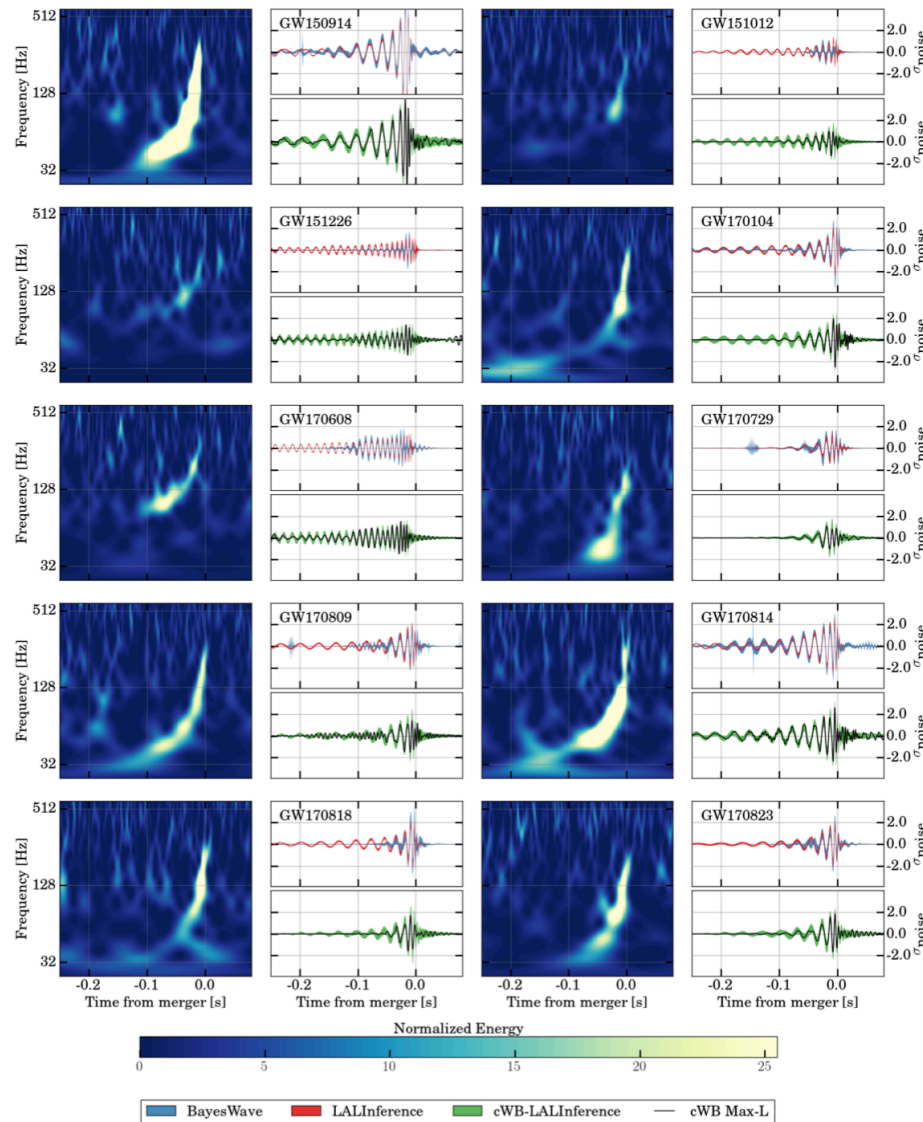


FIG. 10. Time-frequency maps and reconstructed signal waveforms for the ten BBH events. Each event is represented with three panels showing whitened data from the LIGO detector where the higher SNR was recorded. The first panel shows a normalized time-frequency power map of the GW strain. The remaining pair of panels shows time domain reconstructions of the whitened signal, in units of the standard

O1 and O2



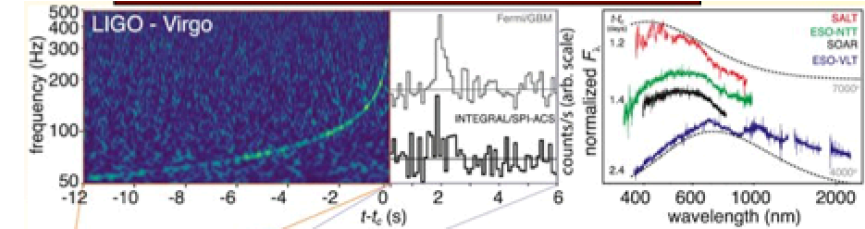
arXiv.org > astro-ph > arXiv:1811.12907

Astrophysics > High Energy Astrophysical Phenomena

GWTC-1: A Gravitational-Wave Transient Catalog of Compact Binary Mergers Observed by LIGO and Virgo during the First and Second Observing Runs

The LIGO Scientific Collaboration, the Virgo Collaboration: B. P. Abbott, R. Abbott, T. D. Abbott, S. Abraham, F. Acernese, K. Ackley, C. Adams, R.

BNS: GW170817



O3

GraceDB — Gravitational Wave Candidate Event Database

HOME	SEARCH	LATEST	DOCUMENTATION	LOGIN
------	--------	--------	---------------	-------

Latest — as of 6 May 2019 20:59:14 UTC

Test and MDC events and superevents are not included in the search results by default; see the [query help](#) for information on how to search for events and superevents in those categories.

Query:

Search for:

Superevent

Search

UID	Labels	t_start	t_0	t_end	FAR (Hz)	<div>UTC</div> Created
S190503bf	DQOK PASTRO_READY EMBRIGHT_READY SKYMAP_READY ADVOK GCN_PRELIM_SENT	1240944861.288574	1240944862.412598	1240944863.422852	1.636e-09	2019-05-03 18:54:26 UTC
S190426c	DQOK EMBRIGHT_READY PASTRO_READY SKYMAP_READY ADVOK GCN_PRELIM_SENT PE_READY	1240327332.331668	1240327333.348145	1240327334.353516	1.947e-08	2019-04-26 15:22:15 UTC
S190425z	DQOK SKYMAP_READY EMBRIGHT_READY PASTRO_READY ADVOK	1240215502.011549	1240215503.011549	1240215504.018242	4.538e-13	2019-04-25 08:18:26 UTC
S190421ar	DQOK EMBRIGHT_READY PASTRO_READY SKYMAP_READY GCN_PRELIM_SENT ADVOK PE_READY	1239917953.250977	1239917954.409180	1239917955.409180	1.489e-08	2019-04-21 21:39:16 UTC
S190412m	DQOK SKYMAP_READY PASTRO_READY EMBRIGHT_READY ADVOK GCN_PRELIM_SENT PE_READY	1239082261.146717	1239082262.222168	1239082263.229492	1.683e-27	2019-04-12 05:31:03 UTC
S190408an	DQOK ADVOK SKYMAP_READY PASTRO_READY EMBRIGHT_READY GCN_PRELIM_SENT PE_READY	1238782699.268296	1238782700.287958	1238782701.359863	2.811e-18	2019-04-08 18:18:27 UTC

The success of GR: Event Horizon Telescope - M87 Pōwehi

THE ASTROPHYSICAL JOURNAL LETTERS

Table of contents

Volume 875

Number 1, 2019 April 10

[Previous issue](#)

[View all abstracts](#)

First M87 Event Horizon Telescope Results. I. The Shadow of the Supermassive Black Hole

The Event Horizon Telescope Collaboration

[Focus on the First Event Horizon Telescope Results](#)

[+View abstract](#) [View article](#) [PDF](#) [ePub](#)

First M87 Event Horizon Telescope Results. II. Array and Instrumentation

The Event Horizon Telescope Collaboration

[Focus on the First Event Horizon Telescope Results](#)

[+View abstract](#) [View article](#) [PDF](#) [ePub](#)

First M87 Event Horizon Telescope Results. III. Data Processing and Calibration

The Event Horizon Telescope Collaboration

[Focus on the First Event Horizon Telescope Results](#)

[+View abstract](#) [View article](#) [PDF](#) [ePub](#)

First M87 Event Horizon Telescope Results. IV. Imaging the Central Supermassive Black Hole

The Event Horizon Telescope Collaboration

[Focus on the First Event Horizon Telescope Results](#)

[+View abstract](#) [View article](#) [PDF](#) [ePub](#)

First M87 Event Horizon Telescope Results. V. Physical Origin of the Asymmetric Ring

The Event Horizon Telescope Collaboration

[Focus on the First Event Horizon Telescope Results](#)

[+View abstract](#) [View article](#) [PDF](#) [ePub](#)

First M87 Event Horizon Telescope Results. VI. The Shadow and Mass of the Central Black Hole

The Event Horizon Telescope Collaboration

[Focus on the First Event Horizon Telescope Results](#)

[+View abstract](#) [View article](#) [PDF](#) [ePub](#)

The EHT Collaboration et al.

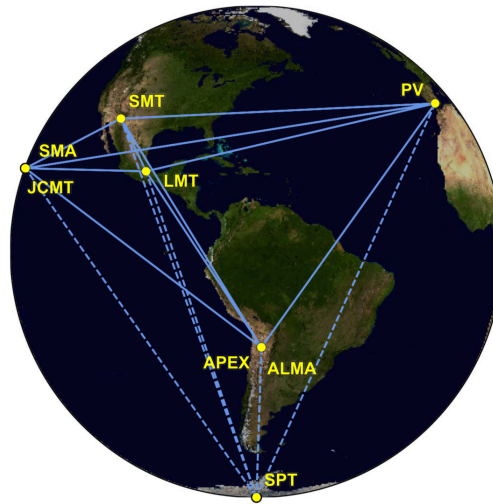


Figure 1. Eight stations of the EHT 2017 campaign over six geographic locations as viewed from the equatorial plane. Solid baselines represent mutual visibility on M87* (+12° declination). The dashed baselines were used for the calibration source 3C279 (see Papers III and IV).

The Universe under the Microscope – Astrophysics at High Angular Resolution
Journal of Physics: Conference Series **131** (2008) 012053
doi:10.1088/1742-6596/131/1/012053

IOP Publishing

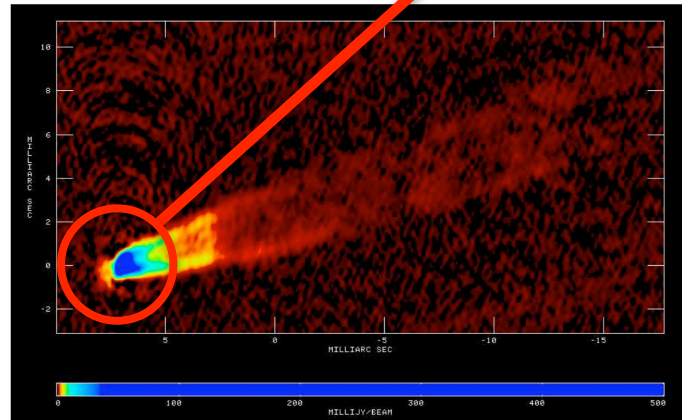


Figure 2. A composite VLBA image of M87 at 43 GHz made by summing the images from the first 9 epochs of the movie project. The resolution is 0.43×0.21 mas elongated along position angle -16° . The image peak is $643 \text{ mJy beam}^{-1}$ and the off-source rms is $0.18 \text{ mJy beam}^{-1}$. Because this image is the sum of several images made at different times, individual features will be blurred out and the jet will appear smoother than it actually is, much like what is seen in a long-exposure photograph of moving water.

The EHT Collaboration et al.

M87* April 11, 2017

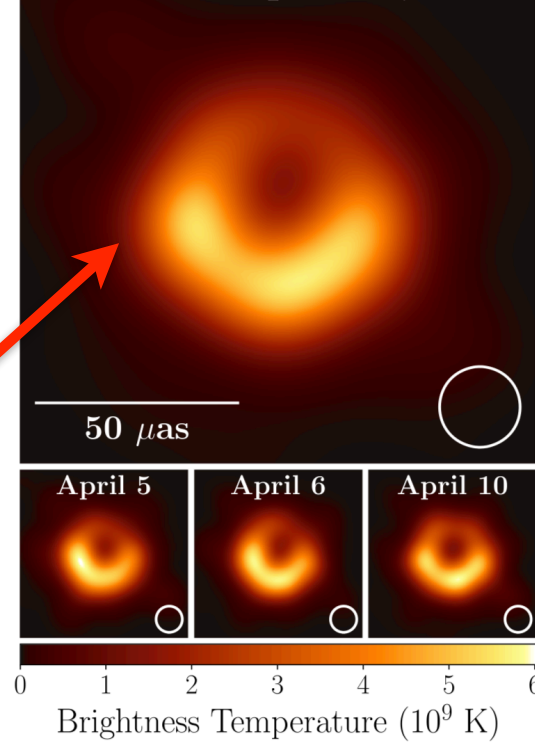
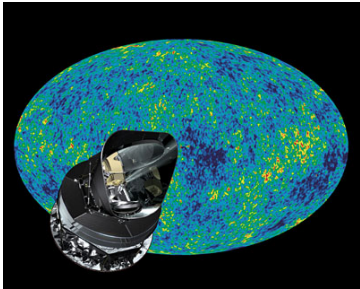
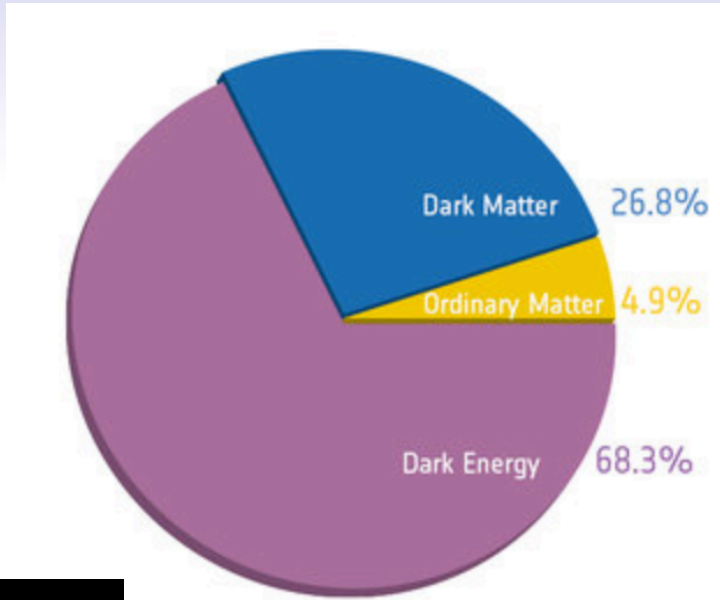


Figure 3. Top: EHT image of M87* from observations on 2017 April 11 as a representative example of the images collected in the 2017 campaign. The image is the average of three different imaging methods after convolving each with a circular Gaussian kernel to give matched resolutions. The largest of the three kernels ($20 \mu\text{as}$ FWHM) is shown in the lower right. The image is shown in units of brightness temperature, $T_b = S\lambda^2 / 2k_B\Omega$, where S is the flux density, λ is the observing wavelength, k_B is the Boltzmann constant, and Ω is the solid angle of the resolution element. Bottom: similar images taken over different days showing the stability of the basic image structure and the equivalence among different days. North is up and east is to the left.

https://iopscience.iop.org/article/10.1088/1742-6596/131/1/012053/pdf?fbclid=IwAR258WA8ofbOCkeFwO3HuaD9yZQ0V4FNE9MGcsmj1r_y229EuuggtJnbNul

slide by Cecilia Gergely

What is the problem with GR then?



After Planck

No dark matter detected:

- 2000 - [MACHO](#) (microlensing)
- 2014, 2016 - [WIMP](#) particles (LUX, PandaX-II, Xenon100)
- 2015 - [Axions](#) (Axion Dark Matter Experiment, Centre for Experimental Nuclear Physics and Astrophysics (CENPA), University of Washington)
- 2016 - [Sterile neutrinos](#) (IceCube)
- 2016 - [Extra dimensions](#) (LHC)
- 2016 - [Supersymmetric particles](#) (LHC)

Dark energy: Cosmological constant?

But this vacuum energy density is [60 orders of magnitude smaller](#) than the theoretical prediction of [zero-point energy](#) in quantum field theory

→ Both DM and DE interact only gravitationally

→ Need to modify GR !

But keep the Solar System and other tests valid !

What else is the problem with GR?

3) Highly non-renormalizable,

can not be formulated as a QFT as for the other fundamental forces,
can not directly be embedded into the standard model of particle physics

4) Early universe inflation requires additional field(s),

best fit with CMB data given by Einstein gravity with an inflaton field
(slow-roll model with a concave potential)

Y. Akrami *et al.* [Planck Collaboration], "Planck 2018 results. X. Constraints on inflation," arXiv:1807.06211 [astro-ph.CO].

5) Tensions in the determination of the Hubble-parameter

CMB measurements from Planck:

$$67.74 \pm 0.46 \text{ km/s/Mpc}$$

SNIa measurements from SHoES21:

$$73.24 \pm 1.74 \text{ km/s/Mpc}$$

GW170817 luminosity distance and optical transient:

$$70.0^{+12.0}_{-8.0} \text{ km/s/Mpc}$$

nature Accelerated Article Preview

LETTER

doi:10.1038/nature24471

A gravitational-wave standard siren measurement of the Hubble constant

The LIGO Scientific Collaboration and The Virgo Collaboration*, The IM2H Collaboration*, The Dark Energy Camera GW-EM Collaboration and the DES Collaboration*, The DLT40 Collaboration*, The Las Cumbres Observatory Collaboration*, The VINROUGE Collaboration* & The MASTER Collaboration*

RESEARCH LETTER

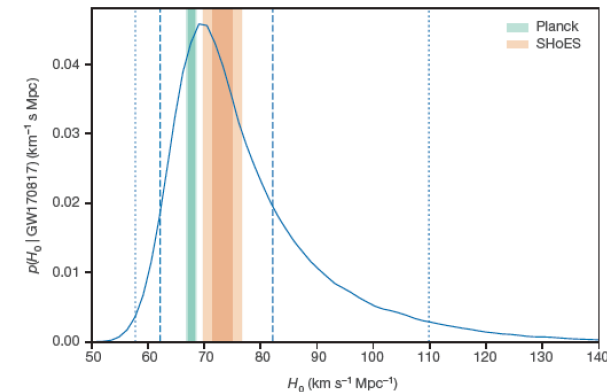


Figure 1 | GW170817 measurement of H_0 . The marginalized posterior density for H_0 , $p(H_0 | \text{GW170817})$, is shown by the blue curve. Constraints at 1σ (darker shading) and 2σ (lighter shading) from Planck²⁰ and SHoES²¹ are shown in green and orange, respectively. The maximum a posteriori value and minimal 68.3% credible interval from this posterior density function is $H_0 = 70.0^{+12.0}_{-8.0} \text{ km s}^{-1} \text{ Mpc}^{-1}$. The 68.3% (1σ) and 95.4% (2σ) minimal credible intervals are indicated by dashed and dotted lines, respectively.

6) Problems in defining gravitational energy-momentum, null boundary terms in the action, occurrence of singularities...

How to go beyond GR?

By relaxing one of the fundamental hypotheses of the Lovelock theorem that makes Einstein theory unique:

- invariance under diffeomorphisms,
(ex: Lorentz-invariance breaking, massive gravity)
- locality,
- pure metric formulation in four space-time dimensions
(add new fields, representing gravity, ex: scalar-tensor theories)

In general they contain one or more extra d.o.f-s, used to

- describe dark energy (fifth force)
- make the theory renormalizable (cure the UV problem of GR)

GW Test 1: Massive graviton modifies dispersion relations

Selected for a **Viewpoint** in *Physics*
 PHYSICAL REVIEW LETTERS

PRL 116, 221101 (2016)



Tests of General Relativity with GW150914

B. P. Abbott *et al.**

(LIGO Scientific and Virgo Collaborations)

(Received 26 March 2016; revised manuscript received 9 May 2016; published 31 May 2016)

For massive graviton

dispersion relations: $E^2 = p^2 c^2 + m_g^2 c^4$

Compton-wavelength: $\lambda_g = h/(m_g c)$

Speed (energy) dependent frequency (wavelength):

$$v_g^2/c^2 \equiv c^2 p^2/E^2 \simeq 1 - h^2 c^2/(\lambda_g^2 E^2)$$

Newtonian potential with Yukawa-corrections

$$\varphi(r) = \frac{GM}{r} \left[1 - e^{-\frac{r}{\lambda_g}} \right]$$

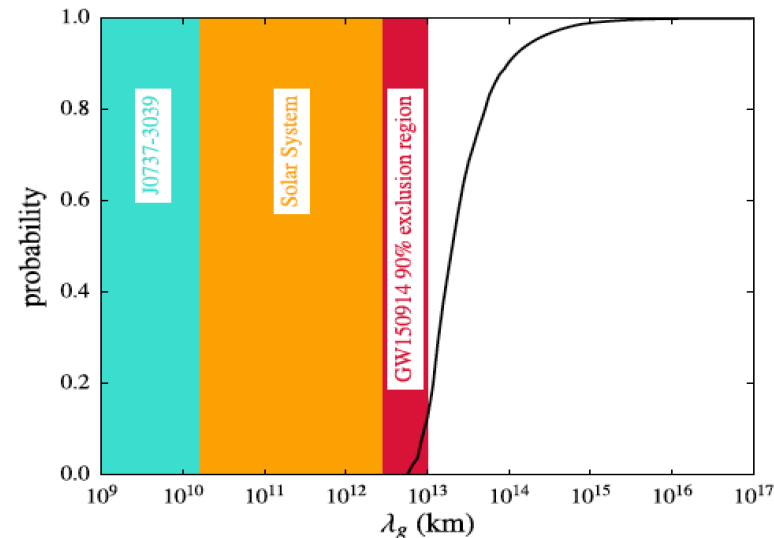
Modified GW phase:

$$\Phi_{MG}(f) = -(\pi D c)/[\lambda_g^2 (1+z)f]$$

(in LCDM, influence on binary dynamics neglected)

C. M. Will, Phys. Rev. D 57, 2061 (1998).

→ From the arrival time-difference between the two LIGO detectors the Compton-wavelength of graviton is constrained from below: 10^{13} km !



$$m_g \leq 1.2 \times 10^{-22} \text{ eV}/c^2.$$

GW Test 2: Local Lorentz-invariance confirmed

Modified dispersion relation:

$$E^2 = p^2 c^2 + A p^\alpha c^\alpha, \alpha \geq 0,$$

S. Mirshekari, N. Yunes, and C. M. Will, *Phys. Rev. D* **85**, 024041 (2012).

Massive graviton theories: $(\alpha = 0, A > 0)$
 Multifractal space-times: $(\alpha = 2.5)$
 Doubly special relativity: $(\alpha = 3)$
 Hořava-Lifšic and extra dimensions: $(\alpha = 4)$

Speed (energy) dependent
 frequency (wavelength):

$$v_g/c = 1 + (\alpha - 1) A E^{\alpha-2} / 2$$

N. Yunes, K. Yagi, and F. Pretorius, *Phys. Rev. D* **94**, 084002 (2016).

Lorentz-invariance violation and massive graviton could be tested in the same time !

Compare to experim. limits on gluon mass
 $< 2 \times 10^{-4} \text{ eV}/c^2$!!

PRL 118, 221101 (2017)

PHYSICAL REVIEW LETTERS

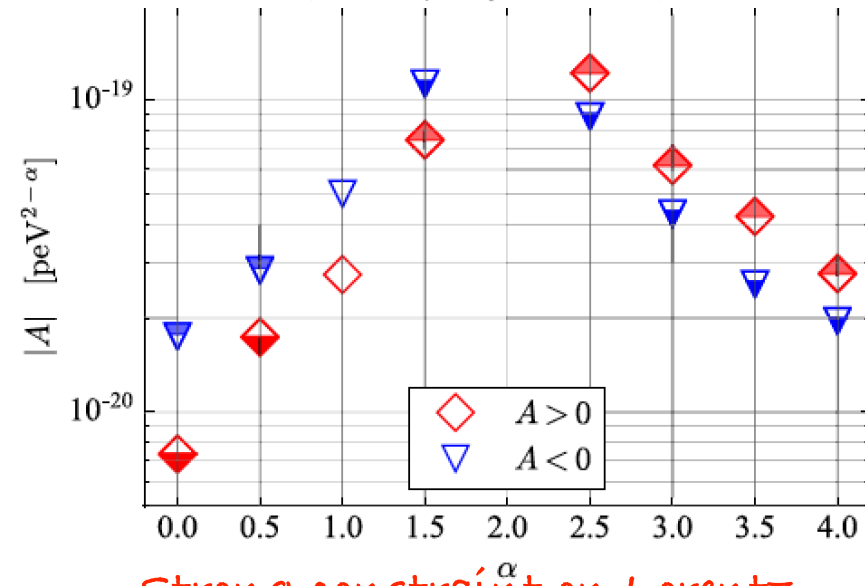


GW170104: Observation of a 50-Solar-Mass Binary Black Hole Coalescence at Redshift 0.2

B. P. Abbott *et al.**

(LIGO Scientific and Virgo Collaboration)

(Received 9 May 2017; published 1 June 2017)



Strong constraint on Lorentz-invariance violation from GW-s !

From first 3 detected GW-s:

$$\lambda_g > 1.6 \times 10^{13} \text{ km},$$

$$m_g \leq 7.7 \times 10^{-23} \text{ eV}/c^2.$$

GW Test 3: PN coefficients checked

Selected for a **Viewpoint** in *Physics*
PHYSICAL REVIEW LETTERS

PRL **116**, 221101 (2016)



Tests of General Relativity with GW150914

B. P. Abbott *et al.**

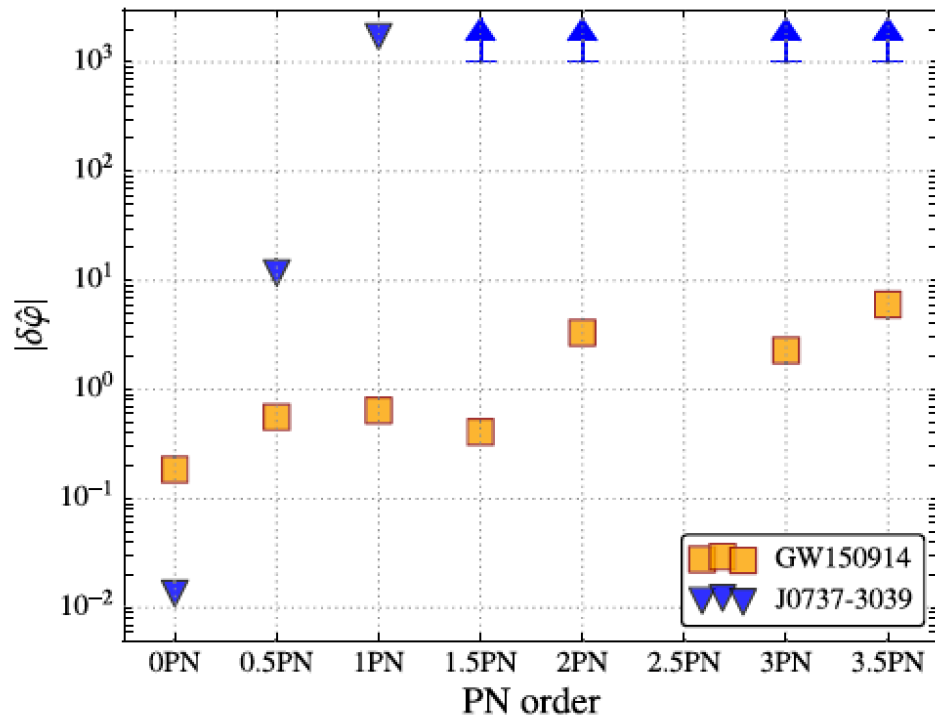
(LIGO Scientific and Virgo Collaborations)

(Received 26 March 2016; revised manuscript received 9 May 2016; published 31 May 2016)

Inspiral-merger-ringdown test:
Modified waveforms in parametric form

GW did not deviate significantly from
GR prediction !
Confirmed the values of the PN
coefficients !

Note: Brans-Dicke theory would generate
a new kind of PN coefficient, still GWs
gave much milder constraint on the BD
parameter, than Solar System tests



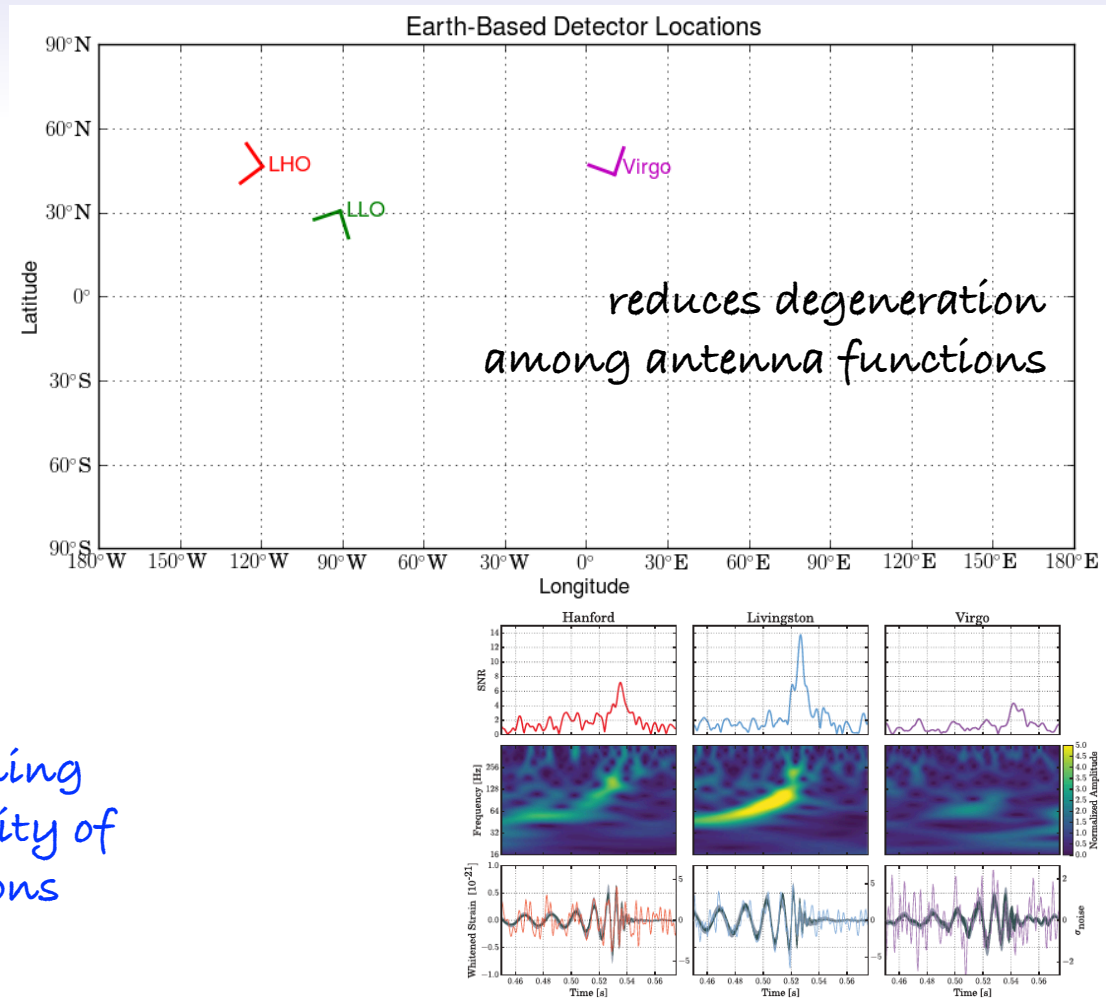
GW Test 4: polarisation check

waveform = $\sum_i \text{antenna function}_i \times \text{polarisation mode}_i$

Preliminary result (toy-model):

GW purely vector
(Bayes-factor 200 times smaller)
GW purely scalar
(Bayes-factor 1000 times smaller
than the one given by GR)
GW purely tensorial

More serious analysis needed, combining
such DoF and looking for the probability of
their coexistence in various compositions



Gravitational scalar-tensor theories

Horndeski-theory: the most general scalar-tensor theory with at most second order dynamics for both the scalar and the metric

G.W. Horndeski, Int. J. Theor. Phys. 10, 363 (1974)

C. Deffayet, G. Esposito-Farese, A. Vikman, Phys. Rev. D 79, 084003 (2009)

C. Deffayet, S. Deser, G. Esposito-Farese, Phys. Rev. D 80, 064015 (2009)

Includes:

GR, quintessence, k-essence, Brans-Dicke, $f(R)$, galileon ...

The effective field theory of cosmological perturbations relies on an action depending of geometric scalars.

It leads to second order dynamics, however space derivatives could be of higher order – it includes Horndeski

J. Gleyzes, D. Langlois, F. Piazza, F. Vernizzi, J. Cosmol. Astropart. Phys. 08 (2013) 025.

QLPV theories / beyond Horndeski theories

Explores the choice of unitary gauge under cosmological symmetries – time is chosen as the scalar field itself

Screening mechanisms: decoupling the scalar d.o.f. below the Solar System scale

Some suppress the scalar charge below the Solar System scale:

Chameleon: J. Khoury and A. Weltman, *Chameleon cosmology*, *Phys. Rev. D* **69** (2004) 044026 [[astro-ph/0309411](#)] [[INSPIRE](#)].

Symmetron: K. Hinterbichler and J. Khoury, *Symmetron fields: screening long-range forces through local symmetry restoration*, *Phys. Rev. Lett.* **104** (2010) 231301 [[arXiv:1001.4525](#)] [[INSPIRE](#)].

Other suppress the scalar field gradient:

k-mouflage: E. Babichev, C. Deffayet and R. Ziour, *k-mouflage gravity*, *Int. J. Mod. Phys. D* **18** (2009) 2147 [[arXiv:0905.2943](#)] [[INSPIRE](#)].

A. Barreira, P. Brax, S. Clesse, B. Li and P. Valageas, *k-mouflage gravity models that pass solar system and cosmological constraints*, *Phys. Rev. D* **91** (2015) 123522 [[arXiv:1504.01493](#)] [[INSPIRE](#)].

P. Brax, L.A. Rizzo and P. Valageas, *k-mouflage effects on clusters of galaxies*, *Phys. Rev. D* **92** (2015) 043519 [[arXiv:1505.05671](#)] [[INSPIRE](#)].

Vainshtein: A.I. Vainshtein, *To the problem of nonvanishing gravitation mass*, *Phys. Lett. B* **39** (1972) 393 [[INSPIRE](#)].

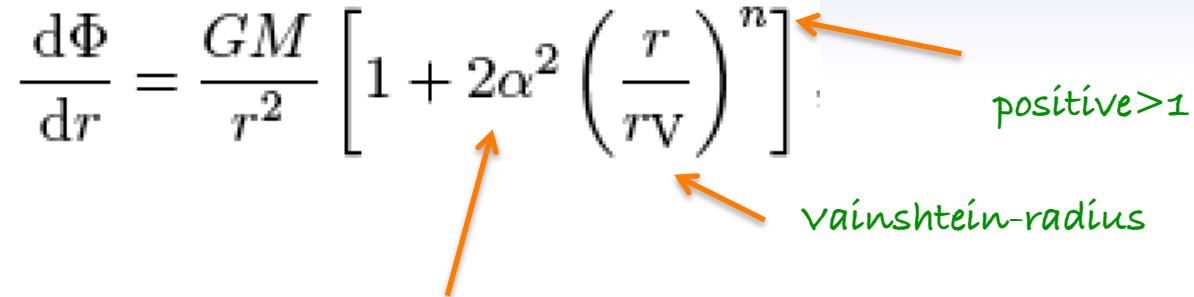
A. Nicolis, R. Rattazzi and E. Trincherini, *The Galileon as a local modification of gravity*, *Phys. Rev. D* **79** (2009) 064036 [[arXiv:0811.2197](#)] [[INSPIRE](#)].

K. Koyama, G. Niz and G. Tasinato, *Effective theory for the Vainshtein mechanism from the Horndeski action*, *Phys. Rev. D* **88** (2013) 021502 [[arXiv:1305.0279](#)] [[INSPIRE](#)].

R. Kimura, T. Kobayashi and K. Yamamoto, *Vainshtein screening in a cosmological background in the most general second-order scalar-tensor theory*, *Phys. Rev. D* **85** (2012) 024023 [[arXiv:1111.6749](#)] [[INSPIRE](#)].

Vainshtein mechanism

The Newtonian force profile of a mass M in Horndeski theories:

$$\frac{d\Phi}{dr} = \frac{GM}{r^2} \left[1 + 2\alpha^2 \left(\frac{r}{r_V} \right)^n \right]$$


Below the vainshtein radius the fifth force fades away

L_5 is disruled by the requirement to recover Newtonian gravity at short distances (Solar System scale)

For the Sun r_V is of order of 10^2 parsecs, difficult to test:

N. Afshordi, G. Geshnizjani and J. Khoury, *Do observations offer evidence for cosmological-scale extra dimensions?*, *JCAP* **08** (2009) 030 [[arXiv:0812.2244](#)] [[INSPIRE](#)].

L. Hui and A. Nicolis, *Proposal for an observational test of the Vainshtein mechanism*, *Phys. Rev. Lett.* **109** (2012) 051304 [[arXiv:1201.1508](#)] [[INSPIRE](#)].

L. Hui and A. Nicolis, *No-hair theorem for the Galileon*, *Phys. Rev. Lett.* **110** (2013) 241104 [[arXiv:1202.1296](#)] [[INSPIRE](#)].

B. Falck, K. Koyama, G.-B. Zhao and B. Li, *The Vainshtein mechanism in the cosmic web*, *JCAP* **07** (2014) 058 [[arXiv:1404.2206](#)] [[INSPIRE](#)].

From GW170817 the GW propagation speed is c

	$c_g = c$	$c_g \neq c$
Horndeski	<p>General Relativity</p> <p>quintessence/k-essence [42]</p> <p>Brans-Dicke/$f(R)$ [43] [44]</p> <p>Kinetic Gravity Braiding [46]</p>	<p>quartic/quintic Galileons [13] [14]</p> <p>Fab Four [15] [16]</p> <p>de Sitter Horndeski [45]</p> <p>$G_{\mu\nu}\phi^\mu\phi^\nu$ [47], Gauss-Bonnet</p>
beyond H.	<p>Derivative Conformal (20) [18]</p> <p>Disformal Tuning (22)</p> <p>DHOST with $A_1 = 0$</p>	<p>quartic/quintic GLPV [19]</p> <p>DHOST [20] [48] with $A_1 \neq 0$</p>
	Viable after GW170817	Non-viable after GW170817

From the time-lag of 1.7 s difference between the speed of gravity and the speed of light:

$$-3 \times 10^{-15} \leq \frac{\Delta v}{v_{\text{EM}}} \leq +7 \times 10^{-16}.$$

[2] [arXiv:1710.05901 \[pdf, other\]](#)

Dark Energy after GW170817

Jose María Ezquiaga (1 and 2), Miguel Zumalacárregui (2 and 3) ((1) Madrid IFT, (2) UC Berkeley, (3) Nordita)

Comments: 9 pages, 3 figures

Subjects: **Cosmology and Nongalactic Astrophysics (astro-ph.CO)**; General Relativity and Quantum Cosmology (gr-qc); High Energy Physics -

[3] [arXiv:1710.05893 \[pdf, other\]](#)

Implications of the Neutron Star Merger GW170817 for Cosmological Scalar-Tensor Theories

Jeremy Sakstein, Bhuvnesh Jain

Comments: five pages, two figures

Subjects: **Cosmology and Nongalactic Astrophysics (astro-ph.CO)**; General Relativity and Quantum Cosmology (gr-qc); High Energy Physics -

[4] [arXiv:1710.05877 \[pdf, ps, other\]](#)

Dark Energy after GW170817

Paolo Creminelli, Filippo Vernizzi

Comments: 5 pages

Subjects: **Cosmology and Nongalactic Astrophysics (astro-ph.CO)**; General Relativity and Quantum Cosmology (gr-qc); High Energy Physics -

Constraints on Horndeski theory from GW170817

GW propagation speed agrees with the speed of light at the order of one part in quadrillionth at low redshifts

1. Theories with dependence of the kinetic term X in the coupling of the Ricci curvature R and Einstein tensor G_{mn} in L_4 and L_5 are disruled
2. L_5 does not depend on ϕ either (except through its derivatives)
3. due to the Bianchi identities, the whole L_5 vanishes

Kobayashi, T.; Yamaguchi, M.; Yokoyama, J., Prog. Theor. Phys. 2011, 126, 511–529.
 De Felice, A.; Tsujikawa, S., JCAP 2012, 007.
 Baker, T.; Bellini, E.; Ferreira, P.G.; Lagos, M.; Noller, J.; Sawicki, I., Phys. Rev. Lett. 2017, 119, 251301.
 Ezquiaga, J.M.; Zumalacarregu, M., Phys. Rev. Lett. 2017, 119, 251304.
 Creminelli, P.; Vernizzi, F. Phys. Rev. Lett. 2017, 119, 251302.

$$L^H = \sum_{i=2}^5 L_i^H, \quad (4.4)$$

where

$$L_2^H = G_2(\phi, X), \quad (4.5)$$

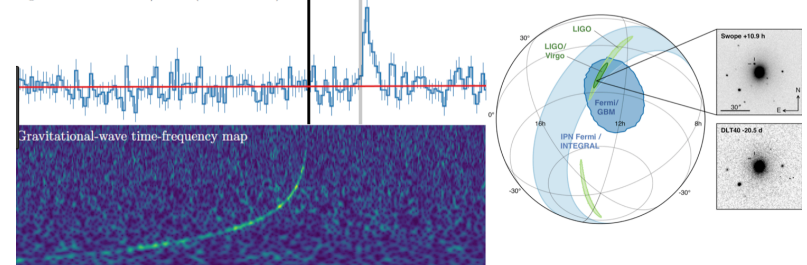
$$L_3^H = G_3(\phi, X) \square \phi, \quad (4.6)$$

$$L_4^H = G_4(\phi, X) R - 2G_{4X}(\phi, X) \times [(\square \phi)^2 - \nabla^a \nabla^b \phi \nabla_a \nabla_b \phi], \quad (4.7)$$

$$L_5^H = G_5(\phi, X) G_{ab} \nabla^a \nabla^b \phi + \frac{1}{3} G_{5X}(\phi, X) [(\square \phi)^3 - 3(\square \phi) \nabla^a \nabla^b \phi \nabla_a \nabla_b \phi + 2 \nabla_a \nabla_b \phi \nabla^c \nabla^h \phi \nabla_c \nabla^a \phi]. \quad (4.8)$$

LIGO, Virgo, and partners make first detection of gravitational waves and light from colliding neutron stars

Lightcurve from *Fermi*/GBM (50 – 300 keV)



Constraints on beyond Horndeski theories from X-ray and lensing profiles

Testing gravity using galaxy clusters: new constraints on beyond Horndeski theories

Jeremy Sakstein, Harry Wilcox, David Bacon, Kazuya Koyama and
Robert C. Nichol

Institute of Cosmology and Gravitation, University of Portsmouth,
Portsmouth PO1 3FX, U.K.

E-mail: jeremy.sakstein@port.ac.uk, harry.wilcox@port.ac.uk,
david.bacon@port.ac.uk, kazuya.koyama@port.ac.uk, bob.nichol@port.ac.uk

Received March 29, 2016

Revised May 24, 2016

Accepted June 27, 2016

Published July 14, 2016

Abstract. The Beyond Horndeski class of alternative gravity theories allow for Self-accelerating de-Sitter cosmologies with no need for a cosmological constant. This makes them viable alternatives to Λ CDM and so testing their small-scale predictions against General Relativity is of paramount importance. These theories generically predict deviations in both the Newtonian force law and the gravitational lensing of light inside extended objects. Therefore, by simultaneously fitting the X-ray and lensing profiles of galaxy clusters new constraints can be obtained. In this work, we apply this methodology to the stacked profiles of 58 high-redshift ($0.1 < z < 1.2$) clusters using X-ray surface brightness profiles from the XMM Cluster Survey and weak lensing profiles from CFHTLenS. By performing a multi-parameter Markov chain Monte Carlo analysis, we are able to place new constraints on the parameters governing deviations from Newton's law $\Upsilon_1 = -0.11^{+0.93}_{-0.67}$ and light bending $\Upsilon_2 = -0.22^{+1.22}_{-1.19}$. Both constraints are consistent with General Relativity, for which $\Upsilon_1 = \Upsilon_2 = 0$. We present here the first observational constraints on Υ_2 , as well as the first extragalactic measurement of both parameters.

JCAP07(2016)019

Constraints on beyond Horndeski theories from X-ray and lensing profiles

$$ds^2 = (-1 + 2\Phi) dt^2 + (1 + 2\Psi) \delta_{ij} dx^i dx^j,$$

$$\frac{d\Phi}{dr} = \frac{GM(r)}{r^2} + \frac{\Upsilon_1 G}{4} \frac{d^2 M(r)}{dr^2}$$

$$\frac{d\Psi}{dr} = \frac{GM(r)}{r^2} - \frac{5\Upsilon_2 G}{4r} \frac{dM(r)}{dr}$$

$$\Upsilon_1 = \frac{4\alpha_H^2}{(1 + \alpha_T)(1 + \alpha_B) - \alpha_H - 1}$$

$$\Upsilon_2 = \frac{4\alpha_H(\alpha_H - \alpha_B)}{5[(1 + \alpha_T)(1 + \alpha_B) - \alpha_H - 1]}$$

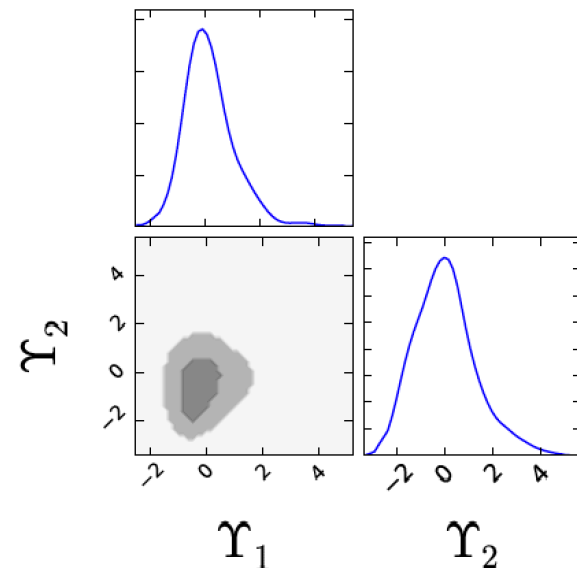
Three parameters appear in them.
Two combinations constrained:

$$\Upsilon_1 = -0.11^{+0.93}_{-0.67} \quad \text{and} \quad \Upsilon_2 = -0.22^{+1.22}_{-1.19}$$

Strong constraints on both the fifth force and lensing parameters, consistent with GR !

Lensing mass is sensitive to $\Phi + \Psi$

Surface brightness measured in X-ray data (hydrostatic mass) sensitive to Φ alone



Constraints from clusters, dwarf stars and propagation speed of GWs

Implications of the Neutron Star Merger GW170817 for Cosmological Scalar-Tensor Theories

Jeremy Sakstein^{1,*} and Bhuvnesh Jain^{1,†}

From GW170817

$$\alpha_T = c_T^2/c^2 - 1$$

is negligible,
2 parameters remain!

Cluster constraints and
dwarf star constraint
(the mass allowing for hydrogen
burning, e.g. for brown dwarf
formation has a maximum)
reevaluated:

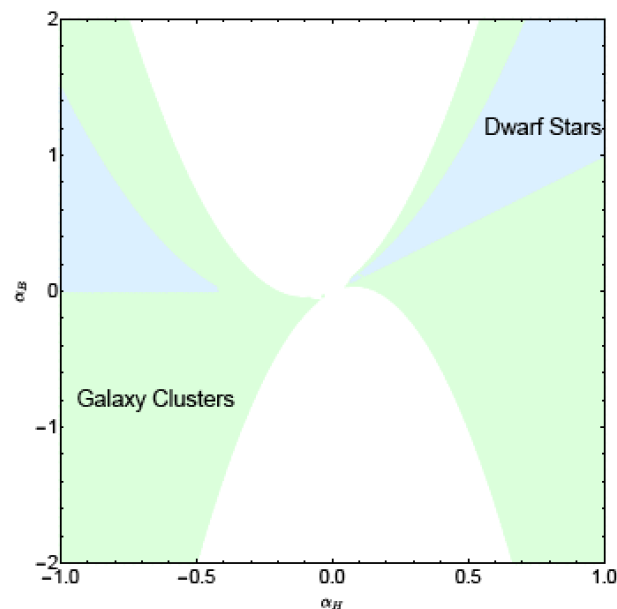


FIG. 1. The excluded regions in the α_H - α_B plane now that c_T is known to be unity with very high precision. The regions excluded by cluster tests and dwarf stars are labeled accordingly.

Freedom in the parameters for deviations from GR still lives

Constraints and their prospects

5 parameters for deviations from Λ CDM of the beyond Horndeski theories:

$$\{\alpha_M, \alpha_K, \alpha_B, \alpha_H, \alpha_T\}$$

Last one is approximately zero due to GW observations

Third and fourth constrained by astrophysical measurements

First gives the running of the Planck mass

- constrain it from time variations of the Newton constant

Second the kinetic term for the scalar

- constrain it from Strong Equivalence Principle violation

They are the parameters of the EFT of dark energy

Constraining them better is one of the goals of the future missions

DESI,

2019

Dark Energy Spectroscopic
Instrument (Arizona)

LSST,

2019

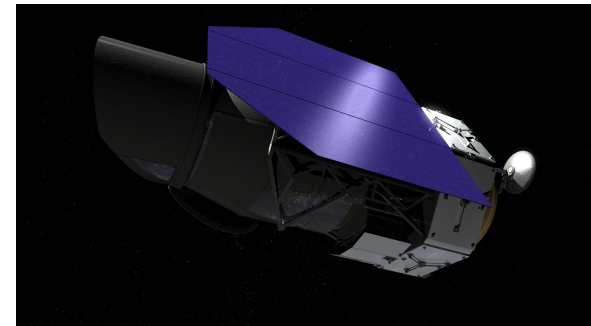
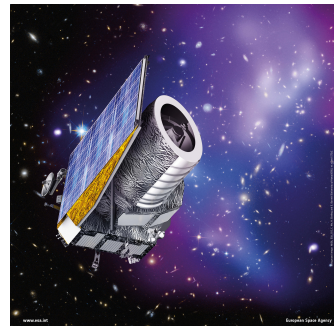
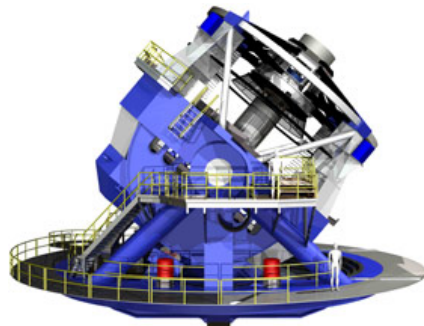
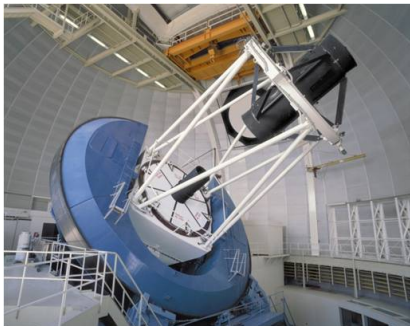
Large Synoptic
Survey Telescope (Chile)

Euclid and WFIRST

2021

Euclid Mission (ESA Wide Field Infrared
& Euclid Consortium) Survey Telescope (NASA)

2025?



Stability analysis example: perturbations of spherically symmetric static BHs in scalar-tensor gravity

EFT action:

$$S^{EFT} = \int dx^4 \sqrt{-\tilde{g}} L^{EFT} (N, M, \mathcal{K}, \mathfrak{K}, K, \varkappa, \mathcal{L}^*, L^*, \lambda^*, R; r)$$

Scalars from embedding variables:

"radial unitary" gauge

$$\mathfrak{K} \equiv \mathcal{K}^a \mathcal{K}_a, \quad K \equiv K^a_a, \quad \varkappa \equiv K^a_b K^b_a, \quad L^* \equiv L^{*a}_a, \quad \lambda^* \equiv L^{*a}_b L^{*b}_a$$

Variations to second order:

$$\begin{aligned} \delta S^{EFT} &= \delta_1 S^{EFT} + \delta_2 S^{EFT} \\ &= \int dx^4 \left(\delta_1 \sqrt{-\tilde{g}} L^{EFT} + \sqrt{-\tilde{g}} \delta_1 L^{EFT} \right. \\ &\quad \left. + \delta_1 \sqrt{-\tilde{g}} \delta_1 L^{EFT} + \delta_2 \sqrt{-\tilde{g}} L^{EFT} + \sqrt{-\tilde{g}} \delta_2 L^{EFT} \right) \end{aligned}$$

variation of the metric determinant:

$$\begin{aligned} \delta \sqrt{-\tilde{g}} &= \delta_1 \sqrt{-\tilde{g}} + \delta_2 \sqrt{-\tilde{g}} \\ &= \sqrt{-\tilde{g}} \left(\frac{\delta_1 N}{\bar{N}} + \frac{\delta_1 M}{\bar{M}} + 2\zeta \right) \\ &\quad + \sqrt{-\tilde{g}} \left[\frac{\delta_1 M \delta_1 N}{\bar{M} \bar{N}} + 2\zeta \left(\frac{\delta_1 N}{\bar{N}} + \frac{\delta_1 M}{\bar{M}} \right) + 2\zeta^2 \right] \end{aligned}$$

conformal transformation

between the 2-dimensional metrics:

$$g_{ab} = e^{2\zeta} \bar{g}_{ab}$$

conformal-factor

Equations of motion for the background

First order variation of the EFT action:

$$\begin{aligned}
 \delta_1 S^{EFT} &= \int d^4x \sqrt{-\tilde{g}} \left\{ [L_N^{EFT} \delta_1 N + L_M^{EFT} \delta_1 M + L_{\mathcal{K}}^{EFT} \delta_1 \mathcal{K} + L_K^{EFT} \delta_1 K \right. \\
 &\quad \left. + L_{\mathcal{L}^*}^{EFT} \delta_1 \mathcal{L}^* + L_{L^*}^{EFT} \delta_1 L^* + L_{\lambda^*}^{EFT} \delta_1 \lambda^* + L_R^{EFT} \delta_1 R] + L^{EFT} \delta_1 \ln \sqrt{-\tilde{g}} \right\} \\
 &= \text{.....cumbersome calculations} \\
 &= \int d^4x \sqrt{-\tilde{g}} \left(\frac{\delta_1 S^{EFT}}{\delta \ln N} \delta \ln N + \frac{\delta_1 S^{EFT}}{\delta \ln M} \delta \ln M + \frac{\delta_1 S^{EFT}}{\delta \ln \mathcal{N}} \delta \ln \mathcal{N} + \frac{\delta_1 S^{EFT}}{\delta \zeta} \delta \zeta \right) \\
 &\quad + \text{total covariant divergencies}
 \end{aligned}$$

Equations of motion:

$$\begin{aligned}
 \frac{\delta_1 S^{EFT}}{\delta \ln N} &= L^{EFT} + \bar{N} L_N^{EFT} + \frac{1}{\bar{M}} \left(\frac{2}{r} + \frac{\bar{N}'}{\bar{N}} + \partial_r \right) L_{\mathcal{L}^*}^{EFT} = 0 \\
 \frac{\delta_1 S^{EFT}}{\delta \ln M} &= L^{EFT} + \bar{M} L_M^{EFT} - \frac{2}{r \bar{M}} \mathcal{F} + \frac{\bar{N}'}{\bar{M} \bar{N}} L_{\mathcal{L}^*}^{EFT} = 0 \\
 \frac{\delta_1 S^{EFT}}{\delta \ln \mathcal{N}} &= \frac{1}{\bar{N} \bar{M}} \left[\partial_r L_{\mathcal{K}}^{EFT} + \frac{2}{r} (L_{\mathcal{K}}^{EFT} - L_K^{EFT}) \right] = 0 \\
 \frac{\delta_1 S^{EFT}}{\delta \zeta} &= 2 \left[L^{EFT} - \frac{1}{\bar{M}} \left(\frac{2}{r} + \frac{\bar{N}'}{\bar{N}} + \partial_r \right) \mathcal{F} - \frac{2}{r^2} L_R^{EFT} \right] = 0
 \end{aligned}$$

arising from the non-orthogonality of the employed double foliation

Scalar perturbations for GLPV black holes: gauge fixing

Unambiguous gauge-fixing for scalar perturbations of both the metric tensor and scalar field on a spherically symmetric, static background.

C. Gergely, Z. Keresztes, L. Á. Gergely, *Gravitational dynamics in 2+1+1 decomposed space-time along nonorthogonal double foliations. Hamiltonian evolution and gauge fixing*, Phys. Rev. D, in press (2019)

Perturbed metric (overbar = unperturbed quantities):

$$ds^2 = -(\bar{N}^2 + 2\bar{N}\delta N) dt^2 + 2\bar{M}\delta\mathcal{N} dt d\chi + 2\delta N_a dt dx^a + (\bar{g}_{ab} + \delta g_{ab}) dx^a dx^b + 2\delta M_a dx^a d\chi + (\bar{M}^2 + 2\bar{M}\delta M) d\chi^2$$

Choices on the background:

R. Kase, L. Á. Gergely, S. Tsujikawa, *Effective field theory of modified gravity on the spherically symmetric background: Leading order dynamics and the odd-type perturbations* Phys. Rev. D 90, 124019 (2014)

$$\bar{N}^a = \bar{M}^a = 0$$

(evolutions perpendicular to $\Sigma_{t\chi}$)

$$\bar{\mathcal{N}} = 0$$

(perpendicular double foliation)

$$\bar{\phi} = \bar{\phi}(\chi)$$

(constant scalar field on $\bar{\mathfrak{M}}_\chi$)

Even/odd decomposition and transformation

Helmholz-type **decomposition** of the **shift vectors** and **metric tensor** into scalars (even), curl-free (even) and divergence-free (odd) parts:

$$\begin{aligned}\delta N_a &= \bar{D}_a P + E_a^b \bar{D}_b Q \\ \delta M_a &= \bar{D}_a V + E_a^b \bar{D}_b W \\ \delta g_{ab} &= \bar{g}_{ab} A + \bar{D}_a \bar{D}_b B + \\ &\quad \frac{1}{2} (E_a^c \bar{D}_c \bar{D}_b + E_b^c \bar{D}_c \bar{D}_a) C\end{aligned}$$

$$E_{ab} = \sqrt{\bar{g}} \varepsilon_{ab}, \quad \varepsilon_{\theta\varphi} = 1$$

Transformations of the metric and scalar
under diffeomorphisms:

(overhat = perturbation after diffeomorphism)

$$\begin{aligned}\mathfrak{L}_\xi \tilde{g}_{ab} &= \delta \tilde{g}_{ab} - \widehat{\delta \tilde{g}_{ab}} \\ \mathfrak{L}_\xi \phi &= \delta \phi - \widehat{\delta \phi} \\ (\xi^t, \xi^\chi, \xi^a &= \bar{D}^a \xi + E^{ba} \bar{D}_b \eta)\end{aligned}$$

$$\begin{aligned}\widehat{\delta \phi} &= \delta \phi - \bar{\phi}' \xi^\chi \\ \widehat{\delta N} &= \delta N - \bar{N} \dot{\xi}^t - \bar{N}' \xi^\chi, \\ \widehat{\delta \mathcal{N}} &= \delta \mathcal{N} - \frac{\bar{N}^2}{2\bar{M}} \xi^{t'} + \frac{\bar{M}}{2} \dot{\xi}^\chi, \\ \widehat{\delta M} &= \delta M + \bar{M}' \xi^\chi + \bar{M} \xi^{\chi'}, \\ \widehat{P} &= P - \bar{N}^2 \xi^t + \dot{\xi}, \\ \widehat{Q} &= Q + \dot{\eta}, \\ \widehat{V} &= V + \bar{M}^2 \xi^\chi + \xi' - \frac{2}{\chi} \xi, \\ \widehat{W} &= W + \eta' - \frac{2}{\chi} \eta, \\ \widehat{A} &= A + \frac{2}{\chi} \xi^\chi, \\ \widehat{B} &= B + 2\xi, \\ \widehat{C} &= C + 2\eta.\end{aligned}$$

in detail

Gauge choice

→ ξ^x to fix $\widehat{\delta\phi} = 0$

→ ξ to fix $\widehat{B} = 0$

→ η to fix $\widehat{C} = 0$

perturbation of 2D-metric = **conformal rescaling**

$$\widehat{g}_{ab} = (1 + \widehat{A})\bar{g}_{ab}$$

Choice of ξ^t : **(1) for orthogonal foliation** → to fix $\widehat{\delta\mathcal{N}} = 0$

$$\xi^t = \int d\chi \frac{2\bar{M}}{\bar{N}^2} \left(\delta\mathcal{N} + \frac{\bar{M}}{2} \dot{\xi}^x \right) + F(t, \theta, \varphi)$$

contains an arbitrary function,

hampering the physical interpretation of perturbations

(2) for non-orthogonal foliations → to fix $\widehat{P} = 0$

unambiguous gauge-choice:

$$\xi^t = \frac{P + \dot{\xi}}{\bar{N}^2}, \quad \xi^x = \frac{\delta\phi}{\phi'}, \quad \xi = -\frac{B}{2}, \quad \eta = -\frac{C}{2}$$

After gauge-fixing the discussion of perturbations possible

even sector: $\widehat{V}, \widehat{A}, \widehat{\delta\mathcal{N}}, \widehat{\delta\mathcal{N}}, \widehat{\delta M}$

Zerilli-type

(only they have first order contributions)

odd sector: \widehat{Q}, \widehat{W}

Regge-Wheeler-type

Comparison of gauge choices

RW

T. Regge, J. A. Wheeler, Stability of a Schwarzschild Singularity, Phys. Rev. 108, 1063 (1957).

GR, time-independent Schrödinger-equation with an effective potential

→ Stable w.respect to perturbations

KMS

T. Kobayashi, H. Motohashi, T. Suyama, Black hole perturbation in the most general scalar-tensor theory with second-order field equations I: The odd-parity sector, Phys. Rev. D 85, 084025 (2012) [arXiv:1202.4893 [gr-qc]].

T. Kobayashi, H. Motohashi, T. Suyama, Black hole perturbation in the most general scalar-tensor theory with second-order field equations II: the even-parity sector, Phys. Rev. D 89, 084042 (2014) [arXiv:1402.6740 [gr-qc]].

Horndeski, stability analysis, only 3 RW variables

KGT

R. Kase, L. Á. Gergely, S. Tsujikawa, Effective field theory of modified gravity on spherically symmetric background: leading order dynamics and the odd mode perturbations, Phys. Rev. D 90, 124019 (2014) [arXiv:1406.2402 [hep-th]].

EFT, odd sector stability analysis, nonphysical variables in the even sector

GKG

C. Gergely, Z. Keresztes, L. Á. Gergely, Gravitational dynamics in 2+1+1 decomposed space-time along nonorthogonal double foliations. Hamiltonian evolution and gauge fixing, Phys. Rev. D, megjelenés alatt (2019).

EFT, 4 RW variables + 1 d.o.f. due to the scalar

	odd perturbations		even perturbations		
	vanishing	physical	vanishing	physical	nonvanishing, nonphysical
RW	$\widehat{C} = 0$	\widehat{Q}, \widehat{W}	$\widehat{B} = \widehat{P} = \widehat{V} = 0$	$\widehat{\delta N}, \widehat{\delta \mathcal{N}}, \widehat{\delta M}, \widehat{A}$	$\widehat{\delta N}, \widehat{\delta \mathcal{N}}, \widehat{P}$
KMS	$\widehat{C} = 0$	\widehat{Q}, \widehat{W}	$\widehat{B} = \widehat{P} = \widehat{A} = 0$	$\widehat{\delta N}, \widehat{\delta \mathcal{N}}, \widehat{\delta M}, \widehat{V}, \widehat{\delta \phi}$	
KGT	$\widehat{C} = 0$	\widehat{Q}, \widehat{W}	$\widehat{B} = \widehat{\delta \phi} = 0$	$\widehat{\delta M}, \widehat{A}, \widehat{V}$	
GKG	$\widehat{C} = 0$	\widehat{Q}, \widehat{W}	$\widehat{B} = \widehat{P} = \widehat{\delta \phi} = 0$	$\widehat{\delta N}, \widehat{\delta \mathcal{N}}, \widehat{\delta M}, \widehat{A}, \widehat{V}$	

Odd sector analysis: Q, W

Odd sector unaffected, by the arbitrary function F , has been discussed in the framework of the orthogonal double foliation:

R. Kase, L. Á. Gergely, S. Tsujikawa, *Effective field theory of modified gravity on the spherically symmetric background: Leading order dynamics and the odd-type perturbations* Phys. Rev. D 90, 124019 (2014)

4th order equations for the evolution of perturbations:

$$\begin{aligned}\bar{D}^2 \Psi^{(1)} &= 0, & \Psi^{(1)} &\equiv a_1 \frac{\partial}{\partial t} \left(\dot{W} - Q' + \frac{2Q}{r} \right) + (a_3 \bar{D}^2 - a_4) W, \\ \bar{D}^2 \Psi^{(2)} &= 0, & \Psi^{(2)} &\equiv \frac{1}{\sqrt{-\bar{g}}} \frac{\partial}{\partial r} \left[\sqrt{-\bar{g}} a_1 \left(\dot{W} - Q' + \frac{2}{r} Q \right) \right] - a_2 \left(\bar{D}^2 + \frac{2}{r^2} \right) Q.\end{aligned}$$

where:

$$a_1 = \frac{L_{\mathfrak{R}}^{\text{EFT}}}{4\bar{N}^2 \bar{M}^2}, \quad a_2 = \frac{L_{\mathfrak{X}}^{\text{EFT}}}{2\bar{N}^2}, \quad a_3 = \frac{L_{\lambda}^{\text{EFT}}}{2\bar{M}^2}, \quad a_4 = L_{\mathfrak{M}}^{\text{EFT}} - \frac{2}{r^2} a_3.$$

Multipolar decomposition

Decomposition in terms of spherical harmonics:

$$\Psi^{(i)}(t, r, \theta, \varphi) = \sum_{l,m} \Psi_{lm}^{(i)}(t, r) Y_l^m.$$

Reduce the differential order to 2 by exploring the identities:

$$r^2 \bar{D}^2 [\Psi_{lm}^{(i)}(t, r) Y_l^m] + l(l+1) [\Psi_{lm}^{(i)}(t, r) Y_l^m] = 0.$$

2nd order system for each mode: $f_l \equiv \sum_m f_{lm} Y_l^m$

2nd order time derivative \rightarrow dynamical eq.

$$\sum_l l(l+1) \Psi_l^{(1)} = 0, \quad \Psi_l^{(1)} \equiv a_1 \frac{\partial}{\partial t} \left(\dot{W}_l - Q'_l + \frac{2}{r} Q_l \right) - \left[a_3 \frac{l(l+1)}{r^2} + a_4 \right] W_l,$$

$$\sum_l l(l+1) \Psi_l^{(2)} = 0, \quad \Psi_l^{(2)} \equiv \frac{1}{\sqrt{-\bar{g}}} \frac{\partial}{\partial r} \left[\sqrt{-\bar{g}} a_1 \left(\dot{W}_l - Q'_l + \frac{2}{r} Q_l \right) \right] + a_2 \frac{l(l+1) - 2}{r^2} Q_l.$$

1st order time derivative \rightarrow Lagrangian constraint

Monopolar, dipolar, higher-order modes

Monopolar mode: trivial, appear only in total divergences in Lag.

Dipolar mode: non-dynamical, constant in time

Higher order mode solutions parametrically given as:

$$Q_l = -\frac{r^2}{a_2(l+2)(l-1)\sqrt{-\bar{g}}}\frac{\partial}{\partial r}(\sqrt{-\bar{g}}a_1Z_l)$$

$$W_l = \frac{a_1r^2}{a_3l(l+1) + a_4r^2}\dot{Z}_l,$$

Second-order correction in the Lagrangian:

$$\delta_2\mathcal{L}_l^{\text{odd}} = \frac{l(l+1)}{(l+2)(l-1)}\sqrt{-\bar{g}}\left[-\frac{a_1^2}{a_3}\dot{Z}_l^2 - \frac{a_1^2}{a_2}Z_l'^2 - a_1(\bar{D}Z_l)^2 - U^H(r)Z_l^2 + \frac{a_1}{a_3}L_{\mathfrak{M}}^{\text{EFT}}W_l\dot{Z}_l\right]$$

where the potential $U^H(r)$ is given by

$$U^H(r) = -a_1\frac{\partial}{\partial r}\left[\frac{1}{\sqrt{-\bar{g}}a_2}\frac{\partial}{\partial r}(\sqrt{-\bar{g}}a_1)\right] - \frac{2a_1}{r^2},$$

last term is l -dependent

—> $L_{\mathfrak{M}}^{\text{EFT}} = 0$ to avoid propagation speed to be dependent (holds in both Horndeski and GLPV)

Ghost modes, stability analysis

- Condition to avoid scalar ghosts: $L_\lambda^{\text{EFT}} < 0$.
- Dispersion relations in the radial direction and along the sphere in the high-frequency / geometrical optics / large wave number limit

$$\omega^2 + \frac{a_3}{a_2} k_r^2 = 0, \quad \omega^2 + \frac{a_3}{a_1} k_\Omega^2 = 0,$$

- Sound velocity-squares :
(defined as change of tortoise coordinate in proper time)

$$\begin{aligned} c_r^2 &\equiv \frac{\bar{M}^2 k_r^2}{\bar{N}^2 \omega^2} = -\frac{\bar{M}^2 a_3}{\bar{N}^2 a_2} = -\frac{L_\lambda^{\text{EFT}}}{L_\chi^{\text{EFT}}}, \\ c_\Omega^2 &\equiv \frac{k_\Omega^2}{\bar{N}^2 \omega^2} = -\frac{a_3}{\bar{N}^2 a_1} = -\frac{2L_\lambda^{\text{EFT}}}{L_{\mathfrak{K}}^{\text{EFT}}} \end{aligned}$$

- Conditions to avoid Laplacian instabilities:

$$L_\chi^{\text{EFT}} > 0, \quad L_{\mathfrak{K}}^{\text{EFT}} > 0.$$

$$\begin{aligned} \mathcal{R} &\equiv {}^{(2)}R^a{}_a, & \mathfrak{M} &\equiv M_a M^a, & \mathfrak{K} &\equiv \mathcal{K}_a \mathcal{K}^a = \mathcal{L}_a \mathcal{L}^a, \\ K &\equiv K^a{}_a, & \chi &\equiv K^a{}_b K^b{}_a, & L &\equiv L^a{}_a, \\ \lambda &\equiv L^a{}_b L^b{}_a. \end{aligned} \tag{3.2}$$

- was applied to both covariantized and covariant galileon models

Summary

- GR is well established, both on theoretical grounds and through observations
- Plagued by necessity to introduce fields, which only interact gravitationally (inflaton, dark matter, dark energy), hence it is de facto modified
- Modifications have to give up on one of these: A) Lorentz-invariance, B) local physics, C) exclusivity of the metric tensor
- GW dispersion relations, propagation speed mostly disrule A) and constrain C), in imposing one parameter of the EFT of dark energy to vanish
- Further astrophysical tests (from X-ray and lensing profiles of galaxy clusters) constrain 2 other parameters of the EFT of dark energy
 → room for deviation from GR at large scale
- The last two parameters to be constrained from time variation of the Newton constant and violation of the Strong Equivalence principle (DESI, LSST, Euclid and WFIRST missions)
- Until then: Theoretical requirement of stability of perturbations. Illustrated here for perturbations of static, spherically symmetric BHs in scalar-tensor theories
- Stability requirements: i) no Ostrogradski ghosts, ii) no kinetic ghosts, iii) no Laplace instabilities, iv) no tachyons
- But other, yet unconstrained modified gravity theories around the corner: generalisations of the teleparallel equivalents of GR

The future of modified gravity?

- GR expresses gravity in terms of space-time curvature and free particles move on geodesics
- But a generic connection has the decomposition:

$$\Gamma^\alpha_{\mu\nu} = \left\{ \begin{smallmatrix} \alpha \\ \mu\nu \end{smallmatrix} \right\} + K^\alpha_{\mu\nu} + L^\alpha_{\mu\nu}$$

Lévi-Civita connection gives GR
 contortion disformation

$$K^\alpha_{\mu\nu} \equiv \frac{1}{2} T^\alpha_{\mu\nu} + T_{(\mu}{}^\alpha{}_{\nu)} \quad L^\alpha_{\mu\nu} \equiv \frac{1}{2} Q^\alpha_{\mu\nu} - Q_{(\mu}{}^\alpha{}_{\nu)}$$

$$T^\alpha_{\mu\nu} \equiv 2\Gamma^\alpha_{[\mu\nu]} \quad Q_{\alpha\mu\nu} \equiv \nabla_\alpha g_{\mu\nu}$$

torsion nonmetricity

- Teleparallel reformulation: no space-time curvature, but torsion or nonmetricity; free particles are subject to gravitational forces
- Modifications of the 3 types of reformulations are inequivalent!

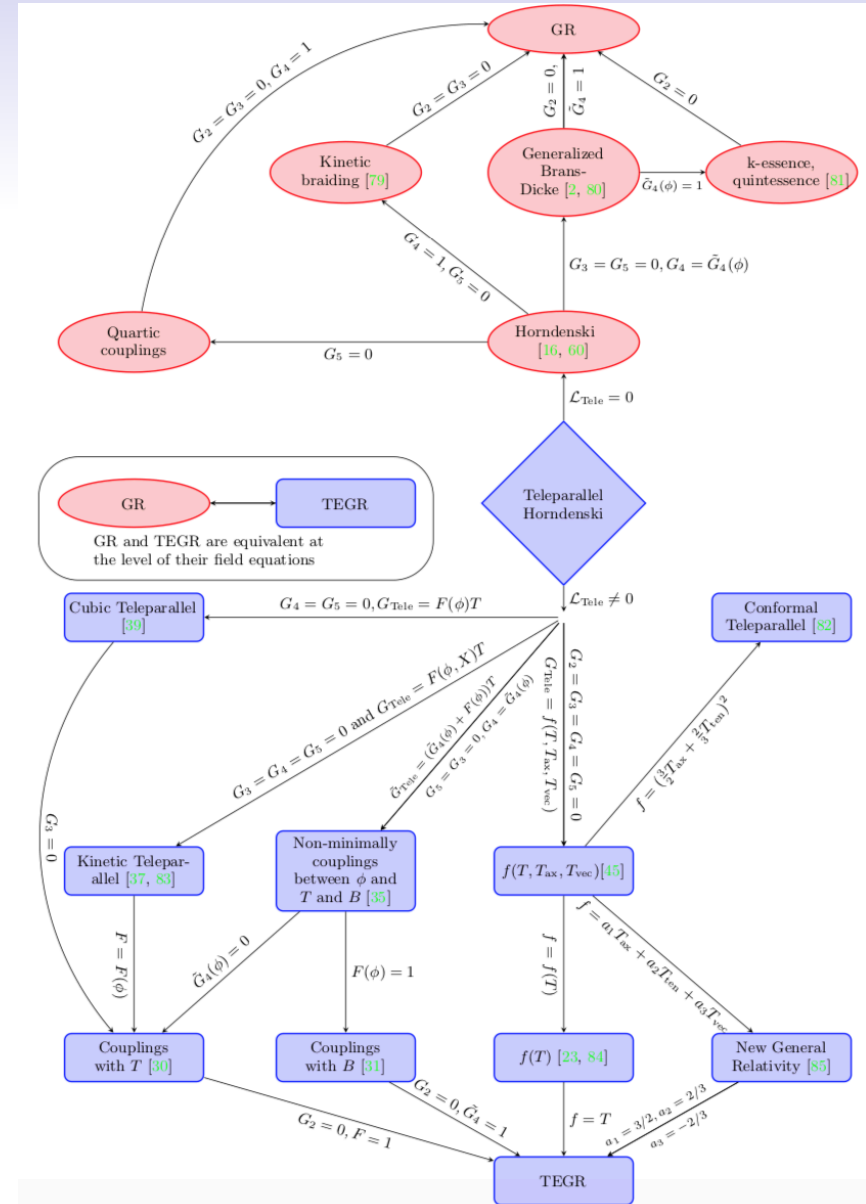



FIG. 1: Relationship between Teleparallel Horndenski and various theories.

CA15117 - Cosmology and Astrophysics Network for Theoretical Advances and Training Actions (CANTATA)

[Home](#) > [Browse Actions](#) > [Cosmology and Astrophysics Network for Theoretical Advances and Training Actions \(CANTATA\)](#)

 cantata-cost.eu

Description

Observations of unprecedented quality reveal a Universe that is at tension with the standard, and very successful description of matter and energy in Physics. Around 95% of the substratum of the Universe is of unknown nature, split into an accreting component (dark matter) and a repelling component (dubbed dark energy). There are auspicious prospects that the combination of state-of-the-art experiments, and theoretical advances will provide us with tools to elucidate this fundamental issue. This Action explores the viewpoint that cosmological observations reveal a degree of incongruous with theory not because of mysterious elements, but because of a need to review and extend Einstein Relativity to scales where it has not been properly tested. So this Action "CANTATA" gathers a team of European leading experts in gravitational physics and cosmology around the timely goal of investigating the extension of Einstein's theory of General Relativity. A program including complementary aspects of theoretical physics, cosmology and astrophysics is put forward which is set to consider, in a coordinated and multidisciplinary way, the build up self-consistent models at the various scales and, in principle, to find out some "*crucial feature*" capable of confirming or ruling out Extended Theories of Gravity with respect to General Relativity. This Action will enhance already existing collaborations and establish an European network with the goal of developing a synergy between expertise and competences, leverage female gender representation, and foster participation of young researchers.